A STUDY OF THE GAMMA RAYS PRODUCED BY THE BOMBARDMENT OF DEUTERIUM WITH PROTONS

by

EUGENE CRITOPH

A THESIS SUBMITTED IN PARTIAL FULFILMENT OF THE REQUIREMENTS FOR THE DEGREE OF

MASTER OF APPLIED SCIENCE

in the Department

of

PHYSICS

We accept this thesis as conforming to the standard required from candidates for the degree of MASTER OF APPLIED SCIENCE

Members of the Department of Physics

THE UNIVERSITY OF BRITISH COLUMBIA

November, 1955

ABSTRACT

The energy of gamma rays from the reaction H^2 (p,γ)He^3 has been measured as a function of incident proton energy in the range of proton energies from 1 to 2 Mev. The results were consistent with the assumption that the He^3 is left in the ground state.

The Doppler shift in gamma ray energy was measured for incident protons of energies 1 Mev. and 1.7 Mev. and was found to be consistent with the value calculated assuming that the He^3 was not slowed down before emission of the gamma ray. This puts an upper limit on the lifetime of the intermediate state of 2×10^{-12} sec.

The angular distribution of gamma rays at an incident proton energy of 1.75 Mev. was of the form $\sin^2\theta + (.025 \pm .007)$, and at incident proton energy of 1.00 Mev. was of the form $\sin^2\theta + (.043 \pm .008)$.

The excitation function, over a range of incident proton energies from 0.25 to 1.85 Mev., is fitted by a function of the form $AE_p^{0.65}$.

ACKNOWLEDGMENTS

I would like to acknowledge the receipt of a National Research Council Bursary for the year 1951-52, without which this work could not have been done.

I would also like to thank Dr. J.B. Warren and Dr. C.A. Barnes, under whose supervision this work was done, and Dr. G.M. Griffiths, who collaborated on this work, for their help and guidance.

TABLE OF CONTENTS

"A Study of the Gamma Rays Produced by the Bombardment of Deuterium with Protons"

I INTRODUCTION

a) Reasons for the Interest in the Reaction $H^2(p,\gamma)He^3$

One of the biggest problems in physics to-day is that of the nature of nuclear forces. At present there is no theory which gives a comprehensive picture of nuclear forces. As a result many problems dealing with nuclei cannot be solved and most predictions concerning nuclear reactions must be based on experience and empirical relations.

The function of the experimental physicist is to obtain as much data as possible on nuclear reactions in order to help the theoretical physicist construct a useful theory of nuclear forces. In so doing, the experimental physicist should attempt to accumulate that data which will be the most useful to the theoreticians. It is reasonable to assume that the most useful data will be that obtained from experiments dealing with the least complex particles and systems of particles. Consequently, most of the experimental work at present in this field concerns reactions involving elementary particles and light nuclei.

The reaction, $H^2(p,\gamma)He^3$, involves only fundamental particles and very light nuclei. Hence it is logical to obtain as much information about this reaction as is feasible. This accounts largely for the interest in this reaction.

There are, however, other reasons for studying this reaction. The first of these is that, based on present knowledge, this reaction seems to provide a source of polarized gamma rays over a range in energy of several Mev. Such a source might be of considerable use in future experiments. Therefore it is desirable to check whether or not this is actually the case. Secondly, this reaction lends itself to the detection and measurement of the Doppler shift in gamma ray energy. Such a shift has been observed once before in $^{a}_{\Lambda}$nuclear reaction (1) and while there is no fundamental importance attached to such an observation it is nevertheless reassuring to check the theory.

b) Previous Work

The reaction, $H^2(p,\gamma)He^3$, was studied by Fowler, Lauritsen and Tollestrup in 1949. (2) They bombarded a thick target of deuterium with protons and detected gamma rays produced in the target.

They measured the energy of these rays as 6.3 ± 0.3 Mev. when the target was bombarded with incident protons having an energy of 1.42 Mev.

They obtained an excitation function for the reaction which yielded a value for the cross-section of $0.74\ E^{0.72} \times 10^{-29}\ cm^2$ for protons of incident energy E. Incidentally this low cross-section accounts for most of the difficulties encountered in studying the reaction.

They also measured the angular distribution of the gamma rays produced with a beam of 1.42 Mev. protons. Their result was that,

$$I_\theta = 0.85 \sin^2\theta + 0.15,$$

where I_θ is the relative flux at the angle θ and,

θ is the angle between the direction of the incident proton beam and the direction of observation.

They felt considerable doubt as to the size of the isotropic component and after more careful work they felt that a better value for the relative isotropic component was $0.04 \pm .02$.

c) Reasons for the Present Study

Since 1949 there has been considerable advance in the equipment and techniques of gamma ray spectrometry. Scintillation crystals have largely replaced Geiger counters for detection and energy-measuring purposes, resulting in vast improvements in energy resolution and efficiency. Hence it was felt that with these new tools and techniques, a more complete and detailed study of the reaction could profitably be made.

II THEORY OF EXPERIMENT

a) Outline of Experiments

The experiments performed in connection with this reaction fall into four main classes: determination of gamma ray energy, measurement of the Doppler shift, measurement of angular distributions, and measurement of excitation function.

The gamma ray energy was measured as accurately as possible for several different incident proton energies, using a single scintillation crystal gamma ray spectrometer. Gamma rays from the reaction F^{19} (p,α,γ) O^{16} were used to calibrate the spectrometer in this region. These calibration gamma rays have well known energies based on a study of the associated particles. (3)

The Doppler shift in gamma ray energy was measured for several different energies of incident protons. The resolution of the spectrometer was good enough to permit this provided considerable care was exercised.

An excitation function was obtained in the range, 250 kev to 1.8 Mev., to check that there were no irregularities which had not previously been detected.

Finally, a careful study of the angular distribution of the gamma rays was made for two incident proton energies; 1 Mev. and 1.7 Mev. Particular attention was paid to the distribution close to the direction of the incident protons. It was felt that this was the most important part of the work and therefore the most time and effort was spent on it.

b) Theory

i) Gamma Ray Energy.

The reaction under consideration is represented as follows:

$$H^2 + p \rightarrow He^3 + \gamma$$

Both the Law of Conservation of Energy and the Law of Conservation of Momentum must hold in this reaction. Assume that the deuterium atom is initially at rest, and let

E_p be the kinetic energy of the incident proton,

E_3 be the kinetic energy of the assembly of proton plus deuteron,

E_γ be the γ-ray energy,

E_r be the recoil energy of the He^3 atom,

m be the mass of the proton,

M_2 be the mass of the deuterium atom,

M_3 be the mass of the helium atom,

Q be the accurate mass difference between He^3 and $H^2 + p$ (assuming both are in the ground state).

Then by the Law of Conservation of Momentum

$$\sqrt{2mE_p} = \sqrt{2M_3E_3}$$

$$\therefore E_3 = \frac{m}{M_3} E_p$$

By the Law of Conservation of Energy

$$E_\gamma = Q + E_p - \frac{mE_p}{M_3} - E_r$$

$$\frac{E_\gamma}{c} = \sqrt{2M_3E_r}$$

or $$E_r = \frac{E_\gamma^2}{2M_3c^2}$$

The formula, to a sufficient degree of accuracy for our purposes, is then,

$$E_\gamma = Q + \left(1-\frac{m}{M_3}\right)E_p - \frac{\left[Q + \left(\frac{M_3 - m}{M_3}\right)E_p\right]^2}{2M_3c^2} \quad \text{------ (1)}$$

Putting in the appropriate values for Q [4], m, M_3 we get,

$$E_\gamma = 5.493 + (2/3)E_p - \frac{[5.493 + (2/3)E_p]^2}{2M_3c^2}$$

where E_γ, E_p and M_3c^2 are in Mev.

Therefore by measuring E_γ for several values of E_p we can get a check on the mass difference and verify that the He^3 nucleus is left in the ground state.

ii) Doppler Shift

When monoenergetic photons are emitted from a body which is moving with respect to an observer, (the photons are monoenergetic in the centre of mass co-ordinates of the body) there is a Doppler Shift in the energy of the photons. That is, the energy as measured by the observer depends upon the angle between the direction of motion of the source and the direction of observation.

Since in our work we will be dealing with velocities which are small with respect to c we can use the non-relativistic formulae for the variation of observed energy with angle. These are [5]

$$E_\gamma' = E_\gamma\left(1 - \frac{v}{c}\cos\theta\right) \quad \text{- - - - - - - - (2)}$$

$$\cos\theta = \cos\theta' \quad \text{- - - - - - - (3)}$$

where v is the velocity of the source with respect to the observer;

c is the velocity of light,

θ is the angle between the velocity vector and the direction of emission in the centre of mass co-ordinate system,

θ' is the angle between the velocity vector and the direction of emission in the observer's system,

E_γ is the photon energy in the centre of mass system,

E_γ' is the photon energy in the observer's system.

In our case, the combination of deuteron and proton has one-third the kinetic energy of the incident proton. Assuming that no energy is lost by collision before emission of a γ-ray, we have

$$\frac{v^2}{c^2} = \frac{2E_p}{9mc^2}$$

where E_p is the incident proton energy

m is the proton mass

and $mc^2 = 931$ Mev.

$$E_\gamma' = E_\gamma \left(1 - \sqrt{\frac{2E_p}{8379}} \cos\theta\right) \qquad \text{---------- (4)}$$

Therefore by measuring the gamma ray energy at various angles from the direction of the incident proton, for various values of E_p, we can check this formula. This would enable us to say something about the time elapsing between the collision with a proton and the emission of a gamma ray.

If we detect a Doppler Shift of the magnitude predicted in equation (4) we will know that the gamma rays were emitted from the bodies before they were slowed by collisions with other atoms in the target. This would enable us to put an upper limit on the lifetime of the intermediate state existing between the

absorption of the proton and the emission of the gamma ray. This upper limit would be of the order of the average time between collisions in deuterium.

iii) Excitation Function

Of interest in all nuclear reactions is a measurement of relative cross-section as a function of incident particle energy. This information is often useful to experimentalists who wish to use a certain type of radiation in experiments and are searching for a suitable source. Also in many cases where resonances occur the information may be used to determine energy levels of the compound nucleus. The previous work done on this reaction showed no resonances and the cross-section increased monotonically with energy over the range studied.

In a reaction of this type in which both the target nucleus and incoming particle are charged we would expect the non-resonant cross-section to increase with energy at low energies. This is due the higher probability that the incoming particle will penetrate the coulomb barrier of the target at higher energies. When the energy of the incident particle is high enough to insure penetration of the coulomb barrier the cross-section should level off. Finally the cross-section should drop off at high energies, where the higher velocity of the incoming particle reduces the time spent in the neighbourhood of the target nucleus and hence the probability that the reaction will take place.

iv) Angular Distributions

It is not within the scope of this thesis to discuss

the general problem of interpretation of angular distributions in nuclear reactions. The reader is referred to French's notes [6] for such a discussion and to M. Verde [7] for a treatment of direct radiative transitions.

III APPARATUS

a) Van de Graaff Generator

The beam of monoenergetic protons used in this experiment was obtained from the University of British Columbia's Van de Graaff generator, which has been described elsewhere. (8,9,10,11)

This machine has several characteristics which make it particularily suitable for studying this reaction. A proton beam current up to 30 μamps, in the energy range from 200 Kev. to 2 Mev. is obtainable. This high current is a necessity due to the low cross-section for the reaction. The energy range is essentially that in which we are interested since background troubles become very serious above 2 Mev. and the yield is extremely low below 200 Kev.

The proton energy may be held constant to within 1 Kev. using the electron gun stabilising system. (10) While this stability is better than is actually needed for this work, it is nevertheless very convenient.

The beam may be focussed in a 1/8" spot or spread out evenly over a circular area $\frac{1}{2}$" in diameter. This is very satisfactory for this work also, since a small spot is needed for doing angular distributions and a diffuse spot was found more convenient in measuring the gamma ray energies.

b) Single Scintillation Crystal Gamma-Ray Spectrometer

1. Theory

i) General.

Many different types of scintillation crystals may

be used for the detection of gamma rays, but sodium iodide crystals with thalium impurity, NaI (Th), are the only crystals, in use at present, which are suitable for the accurate measurement of gamma ray energies. The following discussion will be limited to NaI(Th) crystals and in the case of explicit calculations and curves to one NaI(Th) crystal in particular. This crystal, in the form of a right circular cyliner 2.02" long and with a diameter of 1.76", was the one used in this experiment for the determination of gamma ray energies and also incidentally as a detector in other parts of the work.

When a gamma ray is incident upon a crystal it may pass through unaffected or may be absorbed. There are three mechanisms by which the gamma ray may be absorbed: photo-electric process, Compton process and pair production. In all of these processes at least part of the γ-ray energy is imparted to an electron (also a positron in the case of pair production). The electron subsequently loses energy by the ionization and excitation of atoms of the crystal. These atoms then de-excite and a number of low energy photons ("light" pulse) are emitted. The number of photons emitted (or the intensity of the light pulse) is proportional to the energy of the electron. In turn the spectrum of electron energies arising from a beam of incident monoenergetic gamma rays is dependant on the gamma ray energy. If the spectrum of electron energies arising from a beam of monoenergetic gamma rays is known the gamma ray energy may be deduced. To show how this may be done requires a closer study of the gamma ray absorption processes. Later it will be shown how the electron energy

spectrum arising from the absorption of gamma rays is measured.

ii) Photo-electric process

When an incident gamma ray is absorbed by the photo-electric process all its energy goes into the excitation of an atom. The excited atom emits an electron with kinetic energy equal to the gamma ray energy minus the ionization potential of the electron emitted. Therefore the electron energy spectrum arising from this process is a peak at the incident gamma ray energy minus the most probable ionization potential. This is shown in fig. 1 for a beam of 2.62 Mev. gamma rays from RaTh. The resolution used in plotting these and subsequent theoretical curves was that experimentally determined for the particular crystal mentioned previously. The reason for such a resolution is discussed later. The areas under the curves are normalized to the cross-sections of the various processes at this energy. The curves are only drawn approximately to the expected shape.

iii) Compton Process

When absorbed by the Compton process, the incident gamma ray undergoes a collision with a free electron. This may be considered as an elastic, two-particle collision obeying the Laws of Conservation of Energy and Momentum in the relativistic sense. The electron energy spectrum arising from this process is shown in fig. 1 for the 2.62 Mev. gamma rays from RaTh. The shape of the spectrum and position of the Compton edge depend on the gamma ray energy. (12)

iv) Pair Production

The third mechanism for absorbtion is pair production.

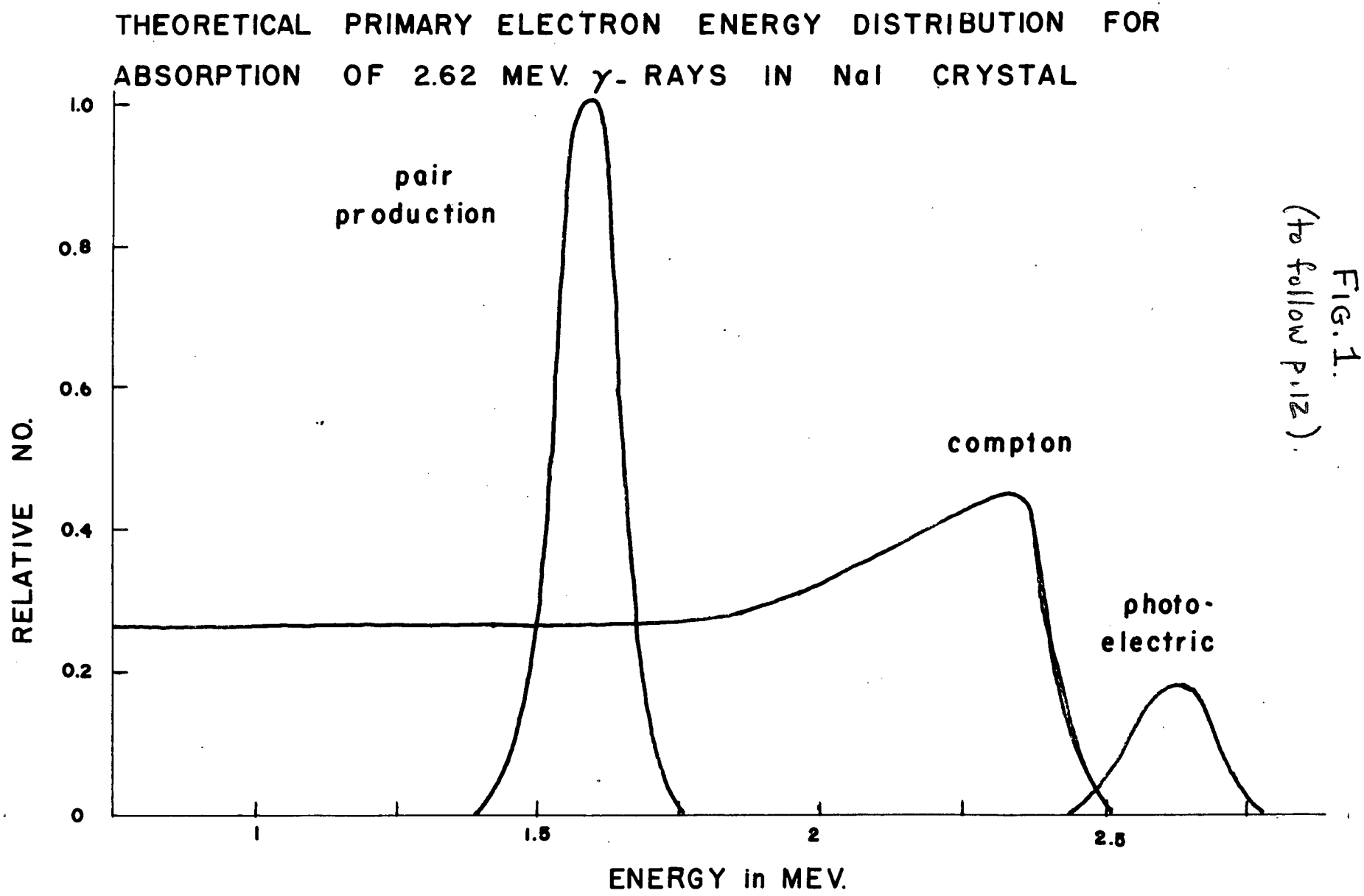

Fig. 1.
(to follow p. 12).

The incident gamma ray can, in the neighbourhood of a nucleus, form an electron and a positron. The energy of the gamma ray minus the energy equivalent of two electron masses (1.02 Mev.) goes into kinetic energy of the positron and the electron. In losing energy these yield a light pulse equivalent to that arising from a single electron with the sum of their kinetic energies. When the positron comes to rest it annihilates with an electron, producing two 0.51 Mev. quanta. The electron energy spectrum due to this process is shown in fig. 1 for the 2.62 Mev. gamma rays from RaTh, assuming both annihilation quantae escape. This is a peak at the gamma ray energy minus 1.02 Mev. Of course pair production takes place only for gamma rays having an energy greater than 1.02 Mev.

v) Resultant Effect of the Three Processes.

If all the secondary gamma rays produced in the Compton process and all the annihilation quanta from the pair production process escaped from the crystal, we would expect the resultant energy spectrum to be the sum of the three spectra due to the three separate processes.

In fact, all the secondary gammas do not escape the crystal. The probability of absorption for an 0.51 Mev. annihilation quanta is approximately 0.6 for this crystal. Therefore the pair production peak is divided into three peaks at (E - 1.02) Mev., (E - 0.51) Mev., and E . The ratio of the areas under these peaks is then roughly .16; .48; .36 as shown in fig. 2. The last peak essentially adds on to the photo electron peak. Some secondary gammas from the Compton process are also absorbed, shifting the Compton edge to a

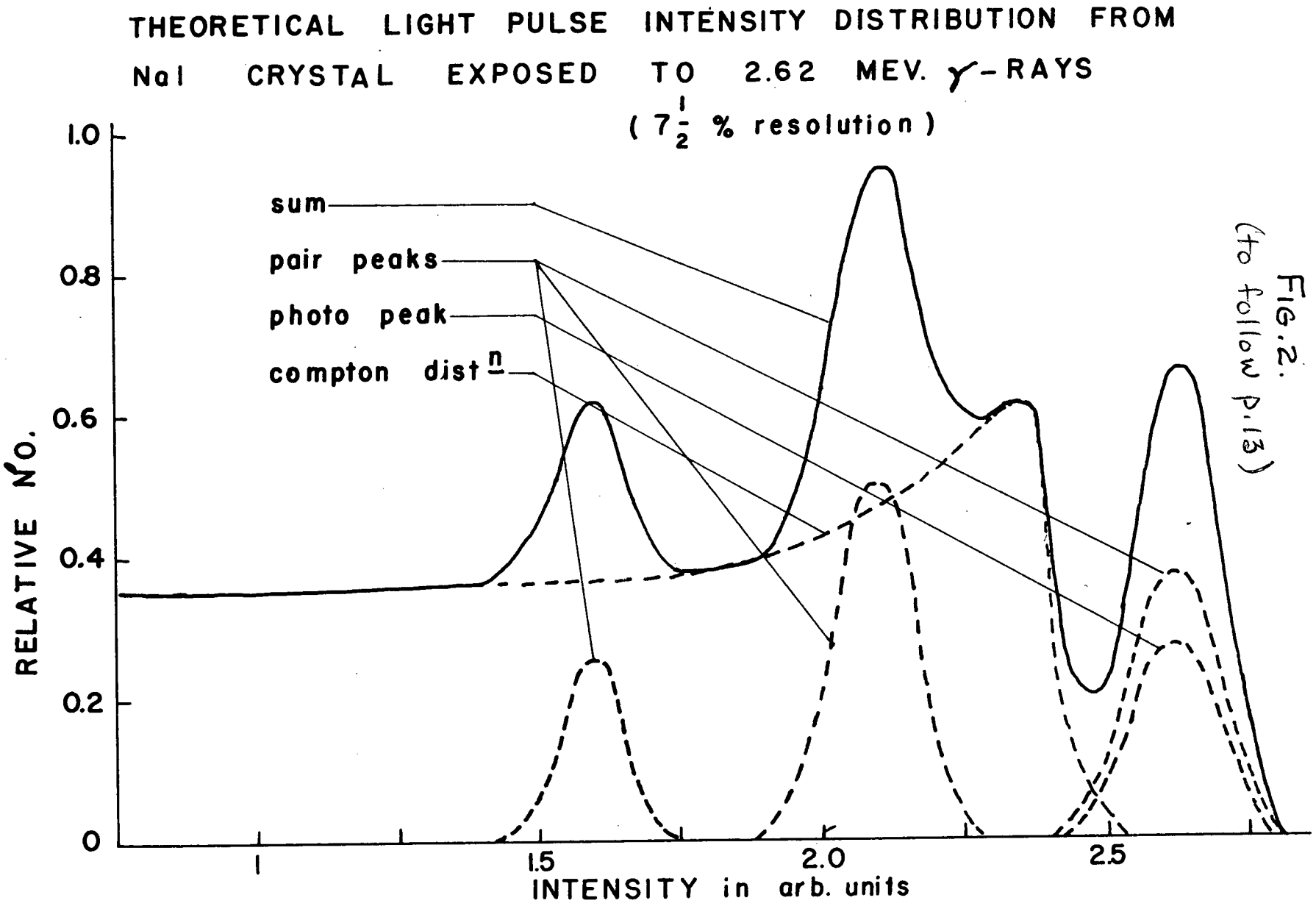

Fig. 2.
(to follow p. 13)

slightly higher energy. The expected resultant electron energy spectrum is shown in fig. 2 after including these refinements.

2. Measurement of Electron Energy Spectrum

As was stated previously, the number of photons (intensity of light pulse) emitted, when an electron is stopped in a NaI(Th) crystal, is proportional to the kinetic energy of the electron. Therefore if the intensity spectrum of light pulses coming from a crystal, which is exposed to gamma rays, is measured, it will have the same shape as the electron energy spectrum. Therefore if we have one or more calibration points (preferrable in the neighbourhood of the gamma ray energy to be measured) we can deduce the gamma ray energy from the light pulse intensity spectrum.

The intensity of the light pulses was measured using a photo-multiplier tube (in our case, EMI 6262). The crystal was mounted on the end of the photo multiplier tube (see fig. 4 and the discussion in the following section) and the assembly made light-tight. The photo multiplier tube then converts the light pulse into a voltage pulse and amplifies it. The voltage pulses were taken from the last or second-to- last dynode and after suitable amplification were fed into an 18-channel, Marconi kick-sorter. Here the voltage pulses were sorted and recorded. The resulting spectrum represents the electron energy spectrum. Therefore from this information the gamma ray energy may be deduced.

A sample experimental spectrum, as displayed on the kick-sorter for the 2.62 Mev. γ-rays from RaTh, is plotted in fig. 3 and may be compared with expected curve in fig. 2. The

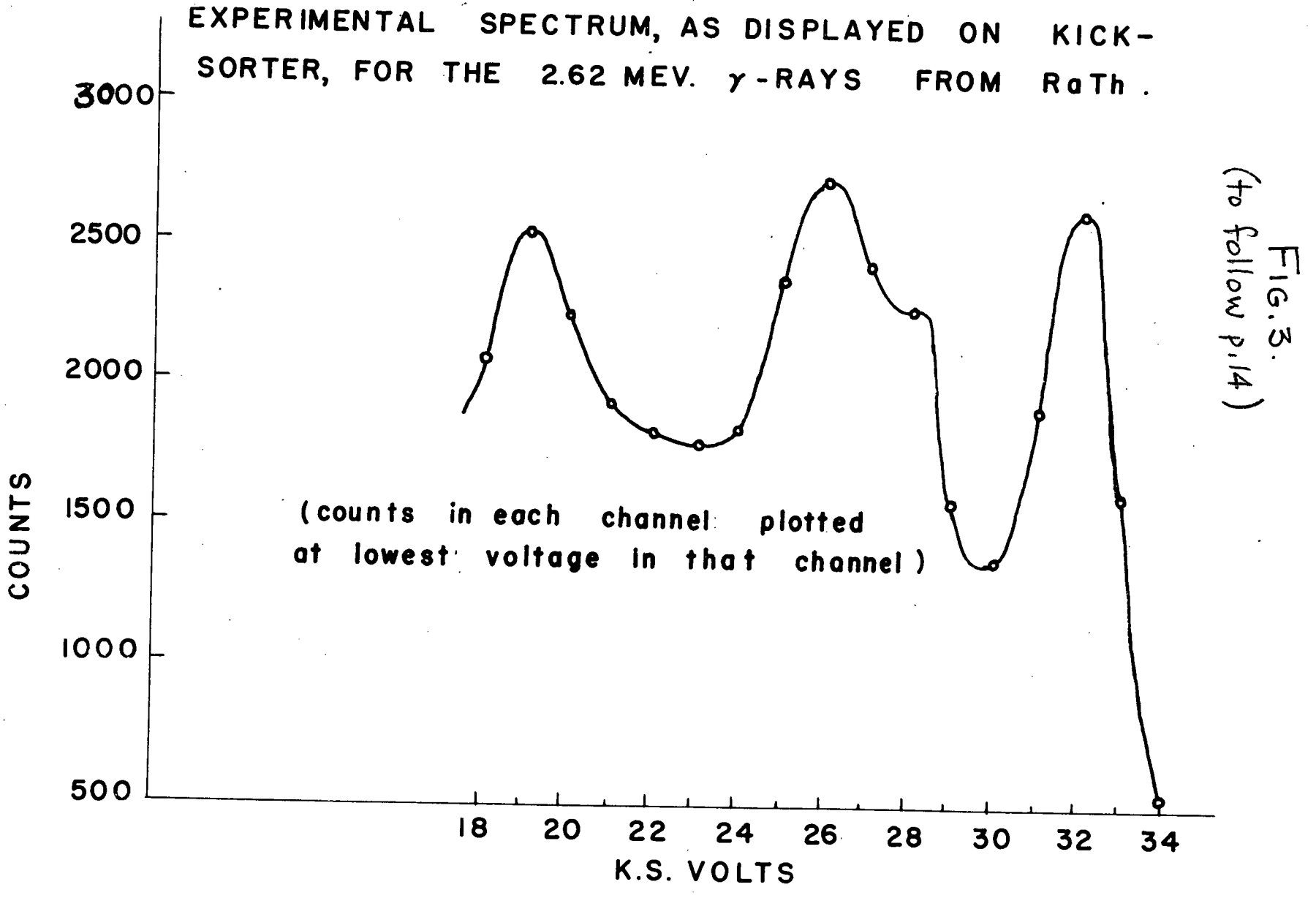

Fig. 3.
(to follow p. 14)

difference in the lower end is due partly to 1.8 Mev. gamma ray contamination.

3. The Technique of Mounting Crystals

The problem of mounting the NaI(Th) crystal is a major one. The crystal must be mounted on the end of a photo multiplier tube with a good optical seal between the crystal and the tube. The whole assembly must be light-tight so that the only light which the tube sees is that arising in the crystal. The difficulties are increased by the fact that NaI(Th) crystals cloud up when exposed to traces of water vapour. This means that the crystal must be kept free from water vapour before, during and after mounting.

"Wet" Mount

A "wet" mount was the first type tried. The crystal was polished well under oil and then put in a thin, loose-fitting aluminium can and the space filled with light mineral oil. The can was then taped securely to the end of an EMI6262 photo multiplier tube so that one face of the crystal pressed tightly against the end of the tube. Care was taken to use enough tape to prevent any oil leaking out. The photo multiplier tube was then taped up to make it light-tight. The resolution obtained with this type of mount was approximately 15% at 2.62 Mev. and was not considered good enough for this work.

"Dry" Mount

The second type of mount tried was a "dry" mount. A dry box was used [13] in which the final steps of mounting could be carried out free from water vapour. The details of

FIG. 4.
(to follow p. 15)

Exploded view

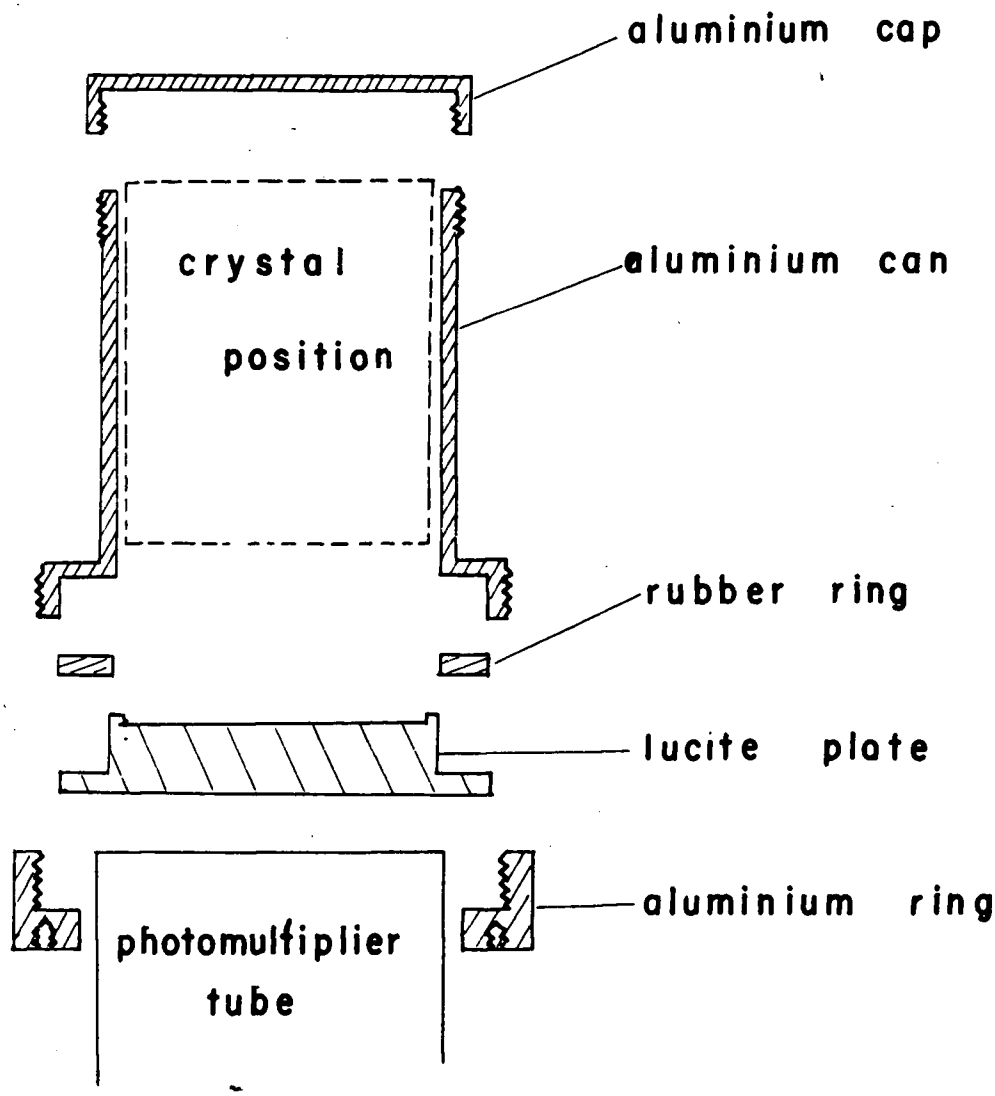

DRY MOUNT FOR NoI CRYSTAL

the mount are shown in fig. 4.

The crystal was given a preliminary polishing, outside the dry box, under oil. Then the remainder of the procedure was carried out inside the dry box. The oil was wiped from the crystal and a final polish administered using blotting paper. Then the crystal was placed on a lucite disk which had been coated with silicone oil of viscosity 2×10^5 centistokes (fig. 4). A good bubble-free contact was made by pressing the crystal firmly down and rotating it. The aluminum cylinder was then put in place and the space along the sides of the crystal packed with MgO powder. A layer of dry MgO powder was put on the top of the crystal and the aluminum cap screwed down. The joints were made light-tight with Black Duco paint.

This formed a permanent unit of a sealed crystal which could be subsequently mounted on any EMI 6262 photo multiplier tube using silicone oil as a light seal between the lucite and the tube. Black tape and plasticene were used to make the assembly of crystal mount and tube light-tight.

MgO powder has a high reflection coefficient for light and it was used to maximize the proportion of the light from the crystal entering the photo multiplier tube and also to keep this proportion constant as the position of the light source changed in the crystal. It also served, incidentally, to absorb any water vapour entering the mount, thereby preventing the crystal from clouding.

This type of mount gave a resolution of approximately 7½% at 2.62 Mev. γ-ray energy, which was considered adequate for this work.

4. Circuitry

A block diagram of the electronics used in the spectrometer is shown in fig. 5. The H.T. supply, which provided the high voltage for the photo multiplier tube, was variable in the range 0 to 2200 volts and was stable to ± 1 volt in 2000 volts after a half-hour, warm-up period. The kick sorter was the Chalk River type [14] produced by Canadian Marconi of Montreal.

5. Linearity, Resolution, and Efficiency

The linearity of the system was checked over a range of photo multiplier H.T. volts and a range of γ-ray energies. An operating voltage of 1100 v. was chosen as a suitable voltage for measuring γ-rays up to 7 Mev. While the linearity over the complete range was only good to a few percent, this was ample since several calibration points were always used close to the gamma ray energy being measured. Over such a restricted range deviations from linearity could not be detected.

The resolution of the spectrometer is defined as the width of a peak (caused by monoenergetic electrons slowing down in the crystal) at half maximum divided by the energy at the peak. There are several factors contributing to this peak width. Due to their finite range some of the electrons escape from the crystal before they lose all their energy. This is called "wall effect" and is of little importance in crystals as large as those used in this study. Statistical fluctuations, in the number of photons arising from the slowing down of an electron of given energy and also in the number of these photons which are effective in producing electrons in

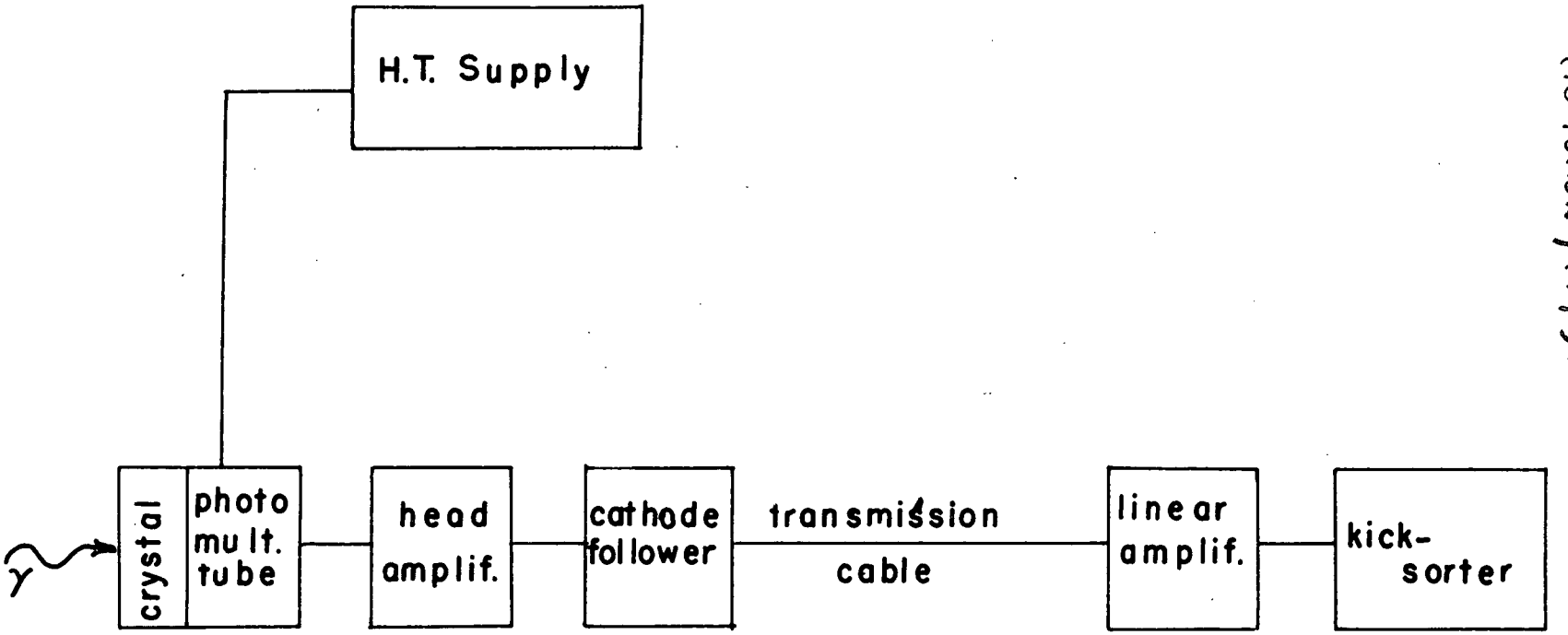

FIG. 5.
(to follow p. 17).

BLOCK DIAGRAM OF ELECTRONICS ASSOCIATED WITH THE γ-RAY SPECTROMETER

the photo multiplier tube, are the most important causes of peak width.

The efficiency of the crystal is of course a function of energy, since the cross-sections for the various absorption processes are functions of energy. The efficiency of this particular crystal is about 33% at 6 Mev.

c) Target Assembly and Target Chamber

1. Tube Assembly

The beam of protons passed from the Van de Graaff proper into an analysing magnet, and then through the tube assembly to the target. The whole system was evacuated, with the pressure being kept below 10^{-5} mm. of mercury. The positioning and design of the components of the tube assembly is shown in fig. 7.

The section adjacent to the magnet box was a 12" length of iron pipe. The purpose of this pipe was to protect the beam from the fringing field of the magnet and hence to eliminate the necessity for realignment of the tube sections and recalibration of slit system as the proton energy was changed.

Next came a sylphon bellows which provided a means of centering the beam on the target. The bellows permitted the target chamber to be moved in any direction perpendicular to the beam.

The next section contained the "sniffers", an auxiliary target (F^{19}), and a quartz shutter. The "sniffers" provided the error signal for the electron gun, stabilizing unit which kept the beam on the target. They merely consisted

of two plates between which the beam passed. If the energy of the beam dropped, the beam struck the ~~lower~~ upper plate, and this sent a signal to the electron gun which lowered the number of electrons sprayed on the upper terminal of the Van de Graaff, thereby raising the voltage and bringing the beam back in position. The ~~top~~ lower plate, of course, sent the reverse signal when struck by the beam. The "sniffer" plates were first made of molybdenum but were later changed to gold to cut down the background. The auxiliary F^{19} target was used for calibration purposes. Since fluorine is a serious contaminant due to its high proton cross-section, precautions were taken in the design to allow it to be completely withdrawn from the beam and protected from any scattered beam. The shutter was made of quartz and was included to permit examination of the beam immediately before it entered the target chamber. It was also used to keep the beam off the target while minor adjustments were being made. The target chamber fitted onto the end of this section.

2. Target Chamber

A detailed drawing of the target chamber is shown in fig. 6. The design of the chamber was dictated by the following requirements:

i) A thin deuterium target was required which was convenient to use and to make. Gas and liquid targets were eliminated on this basis, and a solid, thin heavy water target decided upon. A solid deuterium target was eliminated due to its low freezing point.

FIG. 6.

TARGET CHAMBER

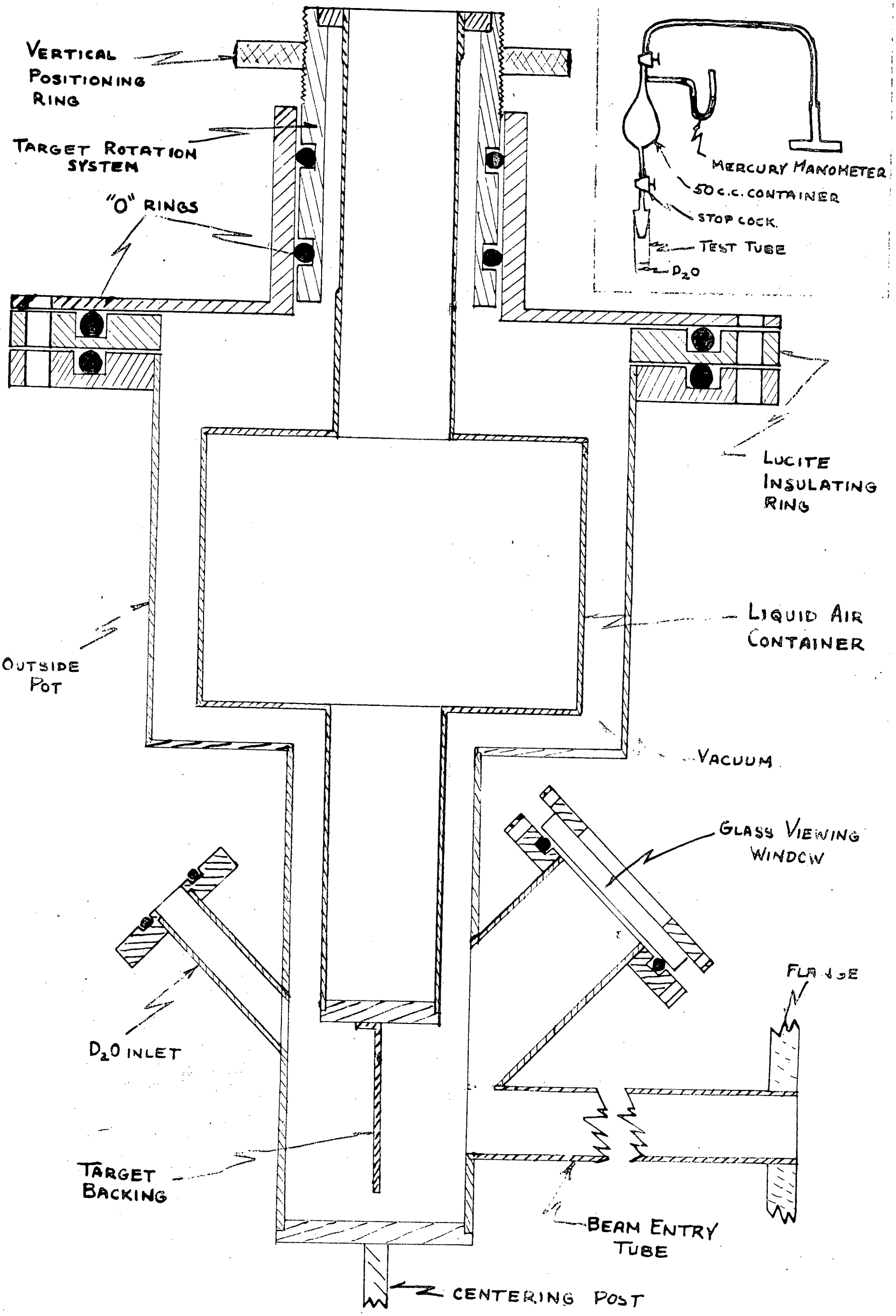

ii) The entering beam had to be well defined and the point at which it struck the target well defined.

iii) Provision had to be made for rotating the target so that effects due to absorption in the backing could be eliminated in the angular distributions.

iv) It was desirable to obtain as large a variation in angle of observation as possible for the angular distributions.

v) The background had to be as low as possible since the cross-section of the reaction being studied was very low.

How these requirements were met can be seen from the drawing in fig. 6 and the discussion which follows. Some of the problems which arose in satisfying the requirements are also discussed.

In order to make the target it was proposed to inject a known volume of D_2O vapour in the vicinity of a cold metal backing. A fraction of the vapour would then freeze on the backing and form the target. The thickness of the target could be regulated by the amount of vapour injected.

Therefore a thin copper sheet was soldered to the end of a cylindrical liquid air container and the whole assembly was surrounded by a larger evacuated chamber. The design was such as to allow a one hour run on one filling of the liquid air container. The general shape as shown in fig. 7 was necessary because the counters had to be very close to the target for some parts of the experiment. A window was inserted to allow the beam positioning and target thickness to be checked. An opening was provided, with a flange and O-ring seal,

for the injection of D_2O vapour. The D_2O dispensing unit is shown in the inset diagram in fig. 6.

The double O-ring seal at the top of the chamber allowed the target to be rotated and also to be moved vertically over a short range. The particular arrangement of this seal was necessary to insure that the O-rings did not get too cold, since this would prevent movement and possibly cause leaks.

The outer chamber was made in two parts for two reasons. In order that the target could be rotated, the diameter of the upper double O-ring seal had to be as small as possible. Once this had been achieved, the outer chamber had to be in two parts so that the target could be put in place and removed easily. Also the target mount had to be insulated from the outer case in order that the current to the target could be measured. This was done by inserting a lucite disk between the two sections of the outer chamber.

Originally it was planned to make the lower section of the outer chamber of aluminium to keep absorption of gamma rays between the target and the counters a minimum. Owing to fabrication difficulties this scheme was dropped and thin brass was used.

The diameter of the tube through which the proton beam entered the target chamber was made small so that as wide a range of angles as possible was available for the angular distribution work. For the same reason the tube was made long enough so that the flange at the end would not seriously restrict the angles available. There were stops at both ends

of this tube. The aperature which the beam encountered first was ¼" in diameter and the one at the target end of the tube was 5/16" in diameter.

In order to keep the background as low as possible, a preliminary study was made of the γ-rays above 2 Mev. arising from the proton bombardment of various materials. Rough excitation functions were run for gold, tungsten, platinum and copper. Tungsten and gold were found to be the best materials as far as background was concerned. Platinum was slightly worse and copper was the worst by a factor of ten. Previous experiments which had been done in this laboratory showed that silver and molybdenum were worse than platinum but far superior to copper.

In the light of this information, the stops were made of pure gold, and the entrance tube to the target chamber was lined with platinum foil. Eventually the "sniffer" plates were also made of gold but this was only for a few of the later runs. At first a sheet of tungsten was attached to the copper backing, on which to deposit the target. However, the heat transfer through the tungsten was so bad that, for beams over 5 μamps. at 1.5 Mev. the target melted and disappeared. Therefore a .020" gold button, 7/8" in diameter, was soldered onto the copper backing and the target was deposited on this button.

3. Counter Holder and Angular Distribution Apparatus

The counter holder and angular distribution apparatus are shown in fig. 7. A central pin was solidly fixed to the bottom of the target chamber and this was the axis about which the moving counter rotated. A large angular scale and pointer

ARRANGEMENT OF EXPERIMENTAL APPARATUS

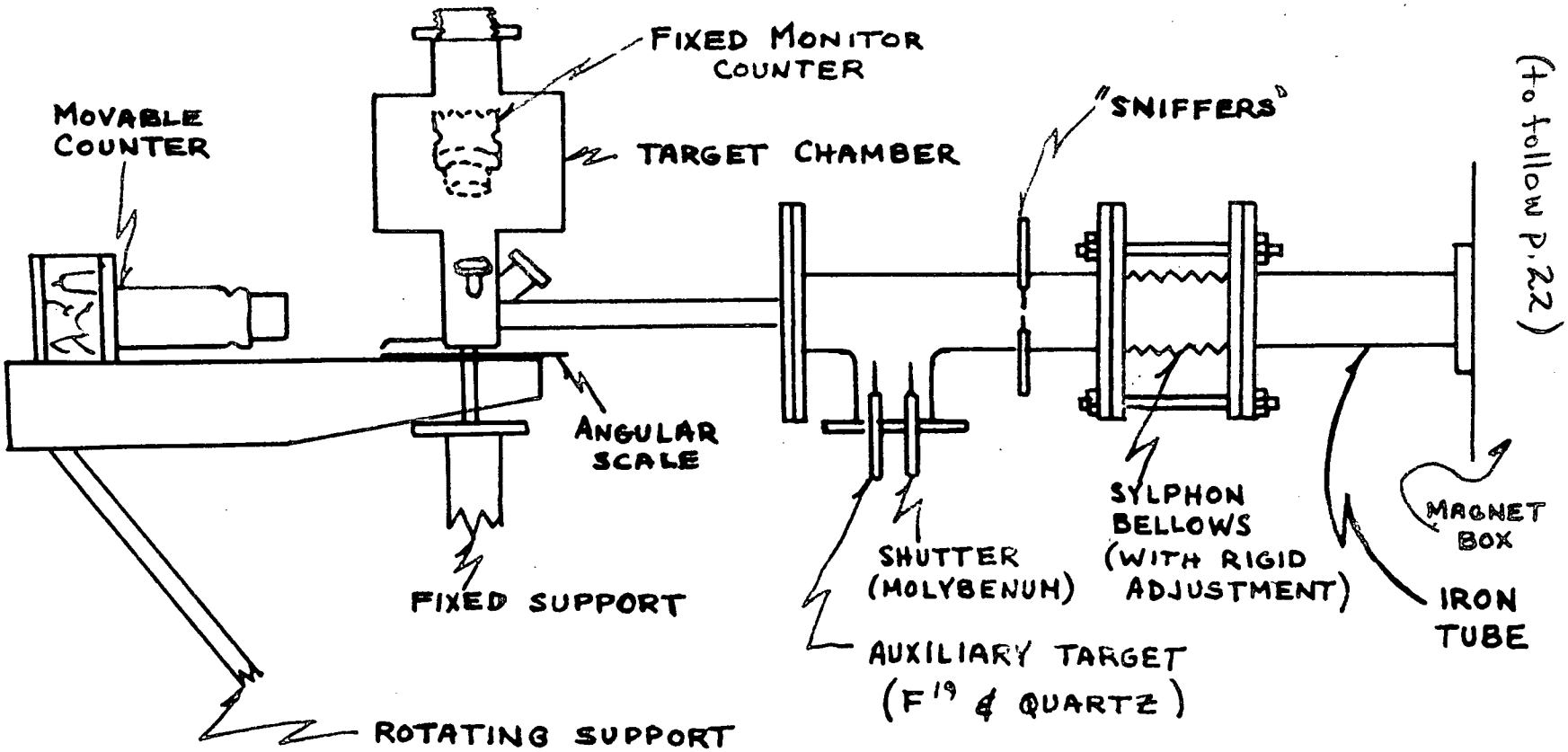

FIG. 7.
(to follow P. 22)

were affixed as shown so that the angle between the direction of observation and the beam could be read directly. The rotating arm, on which the counter sat, was maintained horizontal by a brace and could be clamped in any desired angular position. Adjusting screws allowed the whole stand to be raised or lowered during the lining-up procedure. The counter could be screwed to the counter holder at three definite distances from the centre line of the target. This apparatus allowed an angular accuracy of 1^{o} to be easily maintained.

A monitor counter was firmly fixed to the target chamber as shown in fig. 7. The counter was similar to the main counter but the crystal was somewhat smaller.

4. Arrangement of Apparatus

The arrangement of all the apparatus is shown in fig. 7. Lead shielding between the counting equipment and the Van de Graaff generator was inserted wherever possible to keep down the background.

IV PROCEDURE AND RESULTS

a) Calibration, Checks and Lining-Up of Apparatus

The scintillation counters were first tested and suitable plate volts and amplification factors chosen by studying the γ-rays from RaTh. These were then put in their regular positions with a RaTh source nearby. Spectra were taken for various fields in the Van de Graaff magnet. A slight shift downward of the spectrum with respect to kick-sorter voltage was noted for high magnet fields. Therefore soft iron shields were placed around the photo multiplier tubes and the tests run again. No observable shifts occurred for magnet fields up to the maximum it was planned to use. In all the succeeding work the soft iron shields were always around the photo multiplier tubes.

Lead shielding was wrapped around the sides of the crystals not facing the target, to protect them from soft gamma rays from the Van de Graaff machine. This improved the background quite appreciably.

Part of the equipment associated with the Van de Graaff is a current integrator which was used to measure the total current to the target during any run. Since it was suspected that there might be some electron emission from the target various bias voltages were tried with a steady beam. The current was found to increase with negative bias and decrease with small+bias, thereby substantiating the fear of electron emission. However for positive bias over +90 volts the registered beam current was constant indicating that the +90 volts was enough to prevent electron emission. Therefore

the target was biased to +90 volts during all phases of the work which required a knowledge of the integrated beam current.

Before all runs the following procedure was followed to insure a well-defined and well-centred beam. The quartz shutter was raised and the beam was focussed on it until a uniform spot approximately $\frac{1}{4}$" in diameter was obtained. The tube assembly was then moved about, using the adjusting screws, until the beam looked as though it would pass through the entrance stop. A thick heavy water target was then laid down on the target backing to provide a means of seeing the beam on the target (the thick D_2O target glowed blue where the beam struck it). The quartz shutter was then removed and the spot on the target examined. The line of the target tube was then adjusted, using the clamping screws on the vacuum seal, at the end joining the shutter tube, until the spot was well-defined and circular. The beam focus was then adjusted for maximum current to the target consistent with good definition and shape.

b) Determination of γ -Ray Energy

Method

The target assembly was lined up following the procedure previously outlined. A D_2O target which was estimated to be 60 Kev. thick was then laid down on the target backing. The proton beam was then set to the desired energy by setting the magnetic field in the analysing magnet to the appropriate value and adjusting the Van de Graaff volts until the beam stabilised on the target. Beam currents of the

order of 10-15 microamps. were used.

The gamma ray spectrum from the main crystal was then displayed on the kick-sorter and recorded.

Immediately after this the fluorine target was slipped in to intercept the beam. The fluorine gamma ray spectrum was then recorded. In all the cases done, the proton energy was close enough to a fluorine resonance to get adequate counting rates and spectra without changing the proton energy.

The proton energy was then changed to the next desired energy and the process was repeated.

Results

Graphs of the D_2O and fluorine spectra are shown in fig. 8 for an incident proton energy of 800Kev. Similar spectra were obtained for incident proton energies of 1 Mev. and 1.50 Mev.

The energies and relative abundances of the gamma rays from three of the most important resonances in fluorine are shown in table 1. (16)

TABLE 1

Resonance (E_p)	$E_\gamma \rightarrow$ 6.13 Mev.	6.9 Mev.	7.1 Mev.
873 kev.	0.65	0.24	0.11
1355 kev.	0.53	0.12	0.35
340 kev.	0.96	-	0.04

Using this data and the method previously described, a rough theoretical curve of the expected fluorine spectrum was drawn. This enabled the peaks in the experimental spectrum to

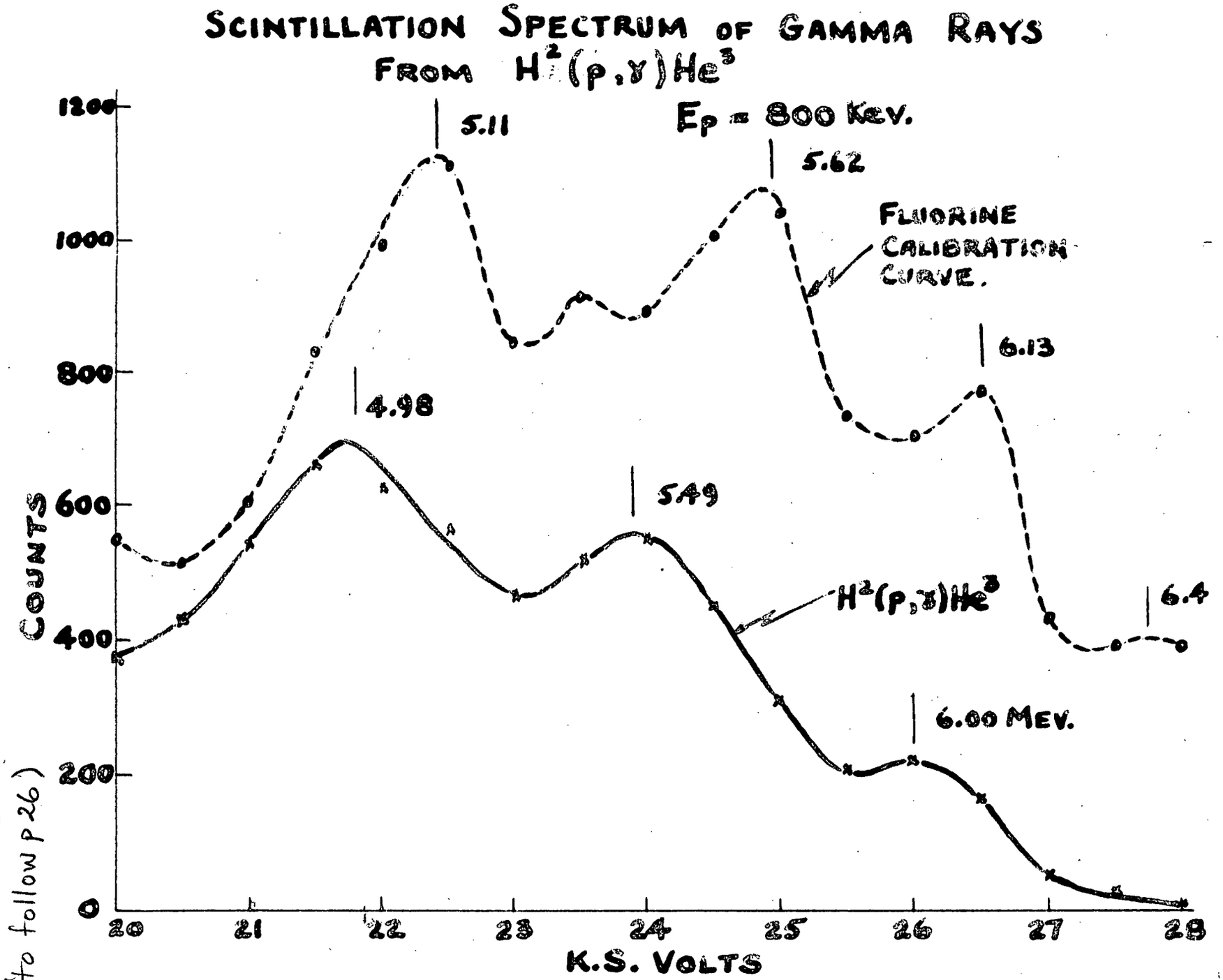

Fig. 8.
(to follow p 26)

be identified and energies assigned to them. (fig. 8). As can be seen from table 1, the 6.13 Mev. gamma ray is the most abundant. Since the peaks from this gamma ray were also in the most suitable energy range they were the ones used in deriving the energy of the γ-ray from deuterum.

The results obtained for E_p = .800, 1.00 and 1.50 Mev. are summarized in table 2.

TABLE 2

E_p Mev.	E_γ Mev.	Targ. Thick. Corr^n Mev.	E_γ Corr. Mev.	Q. Mev.
.800	6.00 ± .04	.03 ± .01	6.03 ± .05	5.50 ± .05
1.00	6.16 ± .04	.03 ± .01	6.19 ± .05	5.52 ± .05
1.50	6.46 ± .04	.03 ± .01	6.49 ± .05	5.49 ± .05
			Avg. Q	5.50 ± .03 Mev.

Sample Calc. for E_p = 800 kev.

As can be seen from fig. 8 the positions and energies of 2 fluorine peaks are:

6.13 Mev. at 26.5 K.S. volts, and

5.11 Mev. at 22.4 K.S. volts.

Hence 1 K.S. volt = 0.249 Mev. (in this range)

The positions of the three pair peaks for the D_2O spectrum are:

Peak	K.S. volts	E_γ
1st Pair (E_γ - 1.02)	21.8	5.98 ± .06
2nd Pair (E_γ - .51)	23.9	5.99 ± .06
3rd Pair (E_γ)	26.0	6.01 ± .06

e.g. E_γ as determined from the 1st pair peak is then:

$$E_\gamma - 1.02 = 5.11 - (22.4 - 21.8)\ (.249)$$
$$= 4.96 \text{ Mev.}$$

$$E_\gamma = 5.98 \pm .06 \text{ Mev.}$$

Where the error quoted is $\frac{1}{2}$ a kick sorter channel. The other values for E_γ shown in table 2 are calculated in a similar manner.

The best value for the γ-ray emitted from deuterium when bombarded with 800 kev. protons, uncorrected for target thickness is $6.00 \pm .06$ Mev.

Q is calculated from formula 1, Section II b (i).

The target thickness was estimated using the following method. The volume, pressure and temperature of the heavy water vapour injected into the system was measured. From this the mass injected can be calculated. It was assumed that the vapour spread uniformly over a sphere whose radius was the distance from the injector to the target. Hence the target thickness in mg./cm^2 could be calculated. Using the figures for stopping cross-section per D_2O molecule from Wenzel & Whaling [15], the target thickness in Mev. was estimated for the incident proton energy. (An upper limit on the target thickness could be determined also by the width of the peaks.) The target thickness estimated in this manner for the above runs was 90 kev. A correction of 45 kev. should be subtracted from the proton energies or $\frac{2}{3}$ (45) = 30 kev. added to the gamma ray energy. In table 2, 30 kev. $\pm$ 10 kev. has been added to the γ-ray energies to correct for the target thickness.

c) Doppler Shift

The apparatus was lined up as previously described.

A fairly thin target was then laid down ($\approx$ 40 kev. thick). The proton beam was then adjusted to the desired energy. A spectrum was taken with the counter at 45° to the direction of the beam. When good statistics had been obtained, the counter was shifted to the 135° position and another spectrum taken. This was repeated several times with readings also being taken once or twice with the counter in the 90° position.

As soon as enough readings had been accumulated, the target was removed by blowing the liquid air out of the pot and warming the target backing. Backgrounds were then taken with the same beam conditions, for the counter in the 45°, 135° and 90° positions. The integrater was used to normalize the background to the regular runs.

Care had to be taken in setting the K.S. channels. Usually the channel width had to be adjusted to show the shift to best advantage. For wide channels the resolution was too poor and for very narrow channels the statistics were bad and also slight errors, in adjusting the channel width showed up more.

The Doppler Shift was measured at 1 Mev. and at 1.7 Mev. Sample curves are shown in figs. 9 and 10 (the backgrounds have been subtracted). The results are tabulated below.

FIG. 9.

DÖPPLER SHIFT AT E_p = 1 MEV.

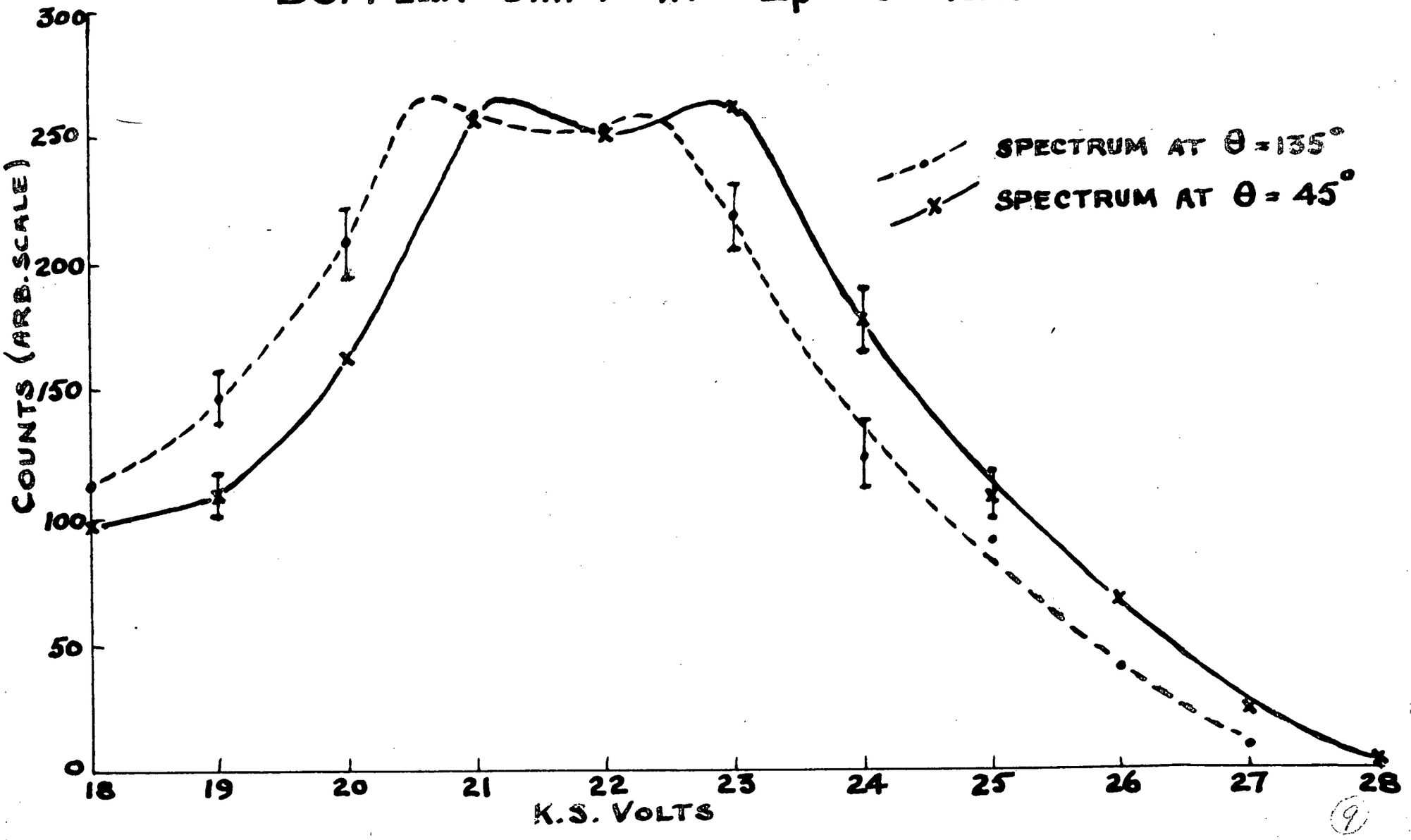

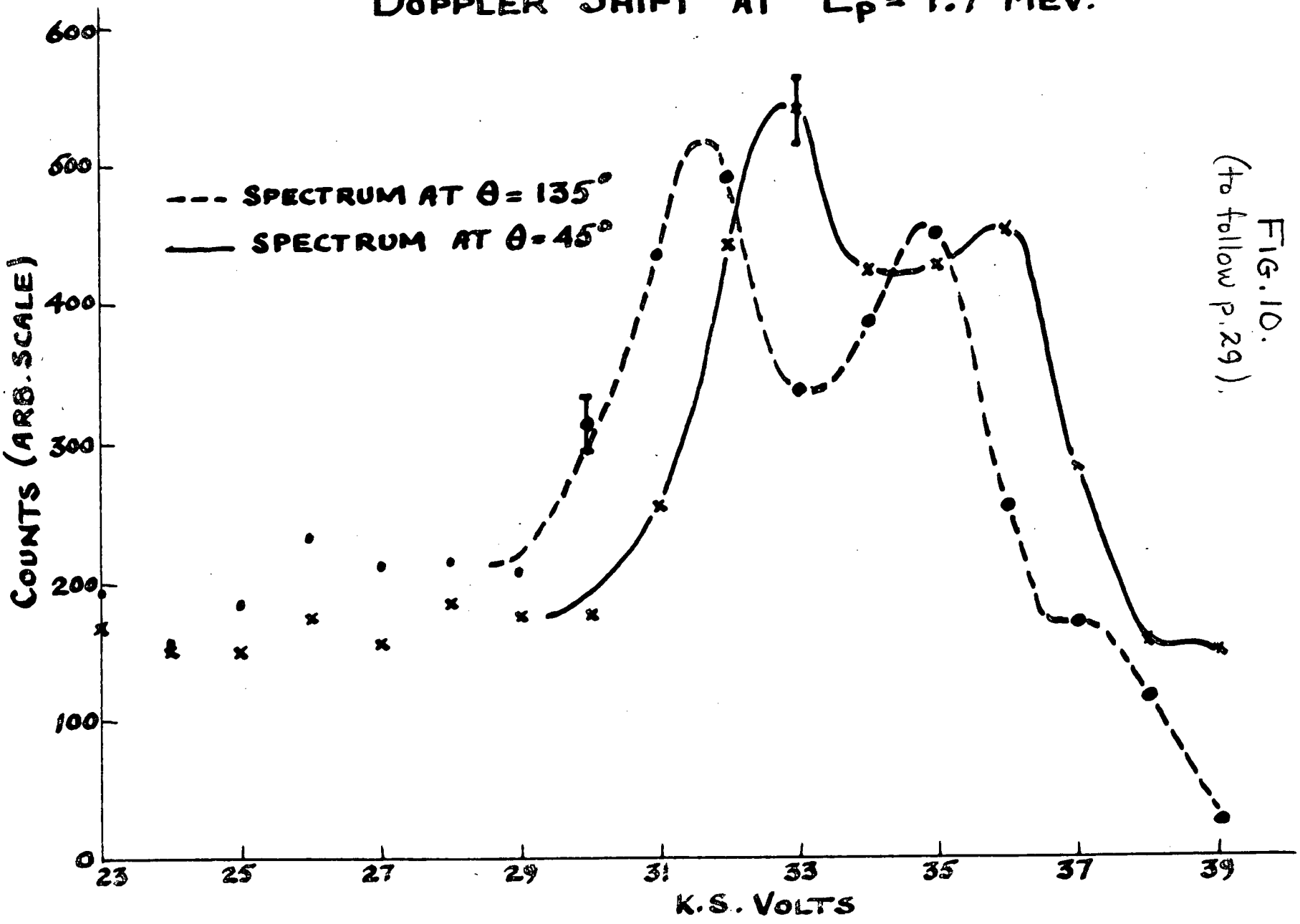

FIG. 10.
(to follow p. 29).

TABLE 3

Doppler Shift from 45° to 135°

Proton Energy	Calculated Value	Observed Value
1 Mev.	133 kev.	135 ± 10 kev.
1.7 Mev.	187 kev.	195 ± 15 kev.

Sample Calculation for Ep = 1 Mev.

The curves in fig. 9 have had the backgrounds subtracted and are normalized so that the corresponding pair peaks are approximately the same height. The displacement between the curves was measured at the Compton edges since this is the steepest part of the curve.

In fig. 9.

Displacement at Compton edges = 0.55 volts.

Energy scale: 23.2 volts corresponds to 5.66 Mev.
i.e. 242 kev./volt.

Doppler Shift = (0.55)(242) = 134 kev.

The probable errors assigned were estimated.

The calculated values in the second column of table 3 were obtained using equation (4) in section II b.

d) Angular Distributions

Method

In taking angular distributions, the main counter was moved, in a horizontal plane, in a circle about the target. The position directly in line with the beam, such that the target was between the beam and the counter, was labelled 0°. All other positions were labelled by their angular displacement from the 0° position as measured either north or south.

The monitor counter was used for this part of the experiment, as well as the movable counter. The pulses from the monitor counter fed into a scaler which was equipped with a descriminator. The descriminator was set at about 4 Mev. so that only pulses above this level were recorded. The monitor counter was fixed at 90°S.

The pulses from the main (movable) counter were fed into the kick-sorter and also into a scaler with descriminator. The descriminator was set so that the count recorded on the scaler was the integral of the spectrum above 4 Mev.

Cosmic ray backgrounds were taken in both the main and monitor counters before the Van de Graaff generator was switched on. This was done by recording the number of counts in both scales during a period of 300 seconds.

The target backing was then put at an angle of 45° to the direction of the beam so that the side facing the beam also faced the monitor counter. A proton beam, of the energy which was to be used for the particular angular distribution being done, was then focussed on the target backing (using the procedure previously outlined).

Background readings were then taken with the movable counter in positions 30° apart between 150°S and 150°N. These readings consisted of time, integrated current, monitor scaler count, main counter scaler count, and kick-sorter readings.

A D_2O target, about 100 kev. thick, was then deposited on the backing. To insure steady beam conditions, the shutter was inserted during this operation rather than shifting the current in the analysing magnet or changing the

Van de Graaff voltage. The beam was then allowed to strike the target and readings of monitor counts, main counter counts, integrated current, time, and kick-sorter counts were taken for the main counter in positions spaced every 15°, between 150°S and 150°N.

The above readings were repeated for the main counter in the 90°S and 90°N positions. The target was then rotated thru 90° and the readings at main counter positions of 90°S and 90°N were repeated. This was done to check the amount of gamma ray absorption in the backing.

The D_2O target was then removed by warming the target backing and the background readings were repeated for the main counter in positions 15° apart between 150°S and 150°N.

The shape of the curve around 0° was obtained with better statistics. This was done by laying down a 100 kev. thick, D_2O target and putting the target perpendicular to the beam. Readings were taken every 5° between 45°S and 45°N. The target was then removed and background readings were taken over the same range of angles.

Results

The cosmic ray background was obtained in counts per unit time for both the monitor counter and the main counter.

Machine background was defined as all background other than cosmic ray background. It was expressed for each counter in counts per unit integrated current. It was in general a function of angular position for the main counter.

For each set of readings the cosmic ray and machine backgrounds were subtracted from the recorded monitor counts and main counter counts. The corrected main counter readings were then normalized to a given monitor count using the corrected monitor counts. Figs. 11 and 12 show some typical results.

The points in Fig. 11 have been corrected for target absorption. This was done by calculating the percentage absorption of gamma rays travelling through the target backing at 45°, from the 4 readings taken at 90°S and 90°N with the target in the two different positions. It was then assumed that the correction varied as the thickness of target backing traversed in going from the target to the counter. This correction was small and after this particular set of results the amount of target backing was reduced. For all subsequent results the absorption in the backing was neglected.

The experimental results are tabulated in Table 4.

The first set of readings taken for each proton energy was used only to verify the general shape of the curve. The value quoted for the isotropic component was obtained from the readings which were taken around 0° with better statistics.

There are two corrections shown in the table which have not yet been explained. The solid angle correction is derived in Appendix A. The neutron correction arose from work done by J. Sample and G.M. Griffiths. They showed that

FIG. 11.

OBSERVED ANGULAR DIST^{N} AT 1.0 MEV.

(CORRECTED FOR TARGET ABSORPTION)

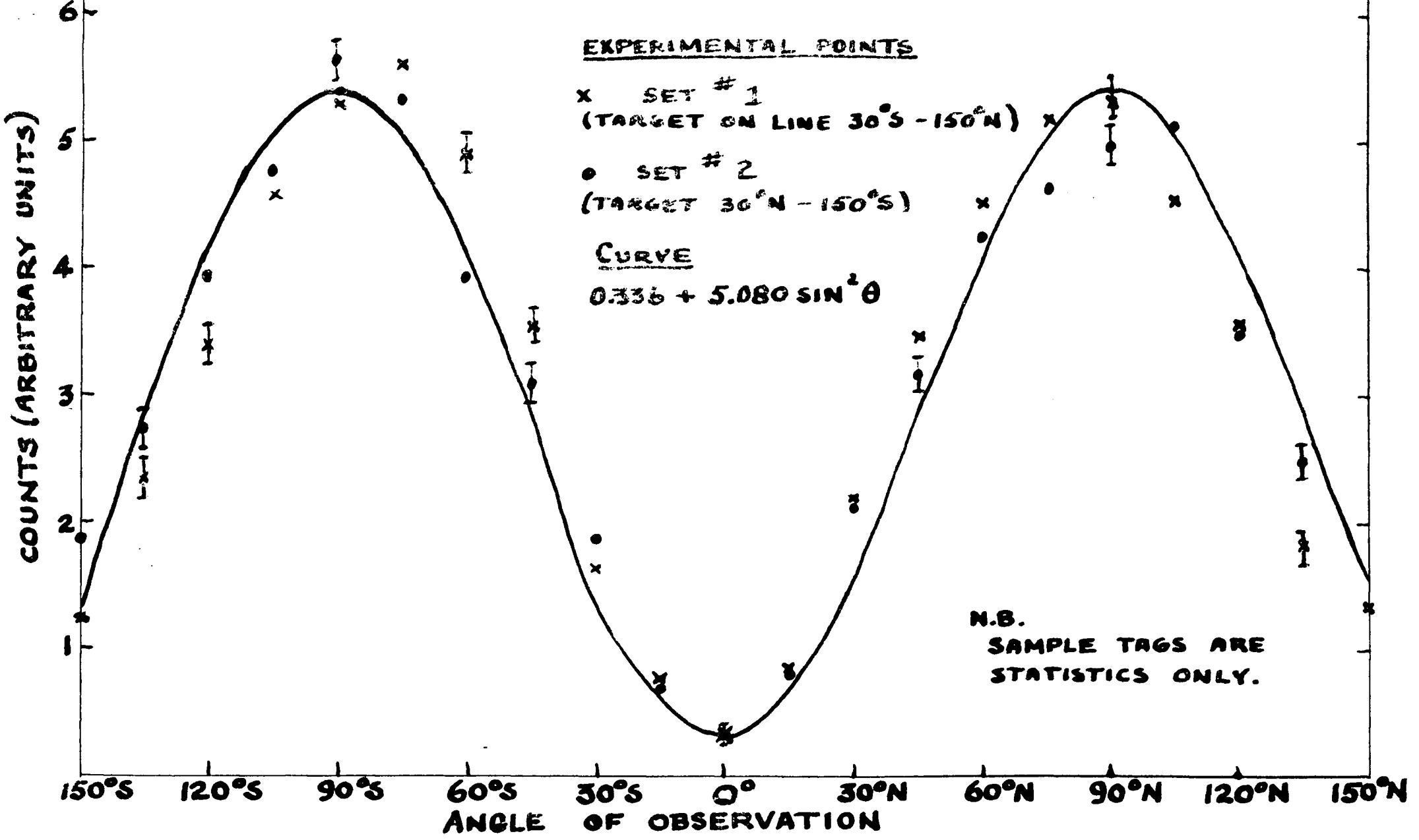

FIG. 12.

ANGULAR DISTRIBUTION AT 1.7 MEV.

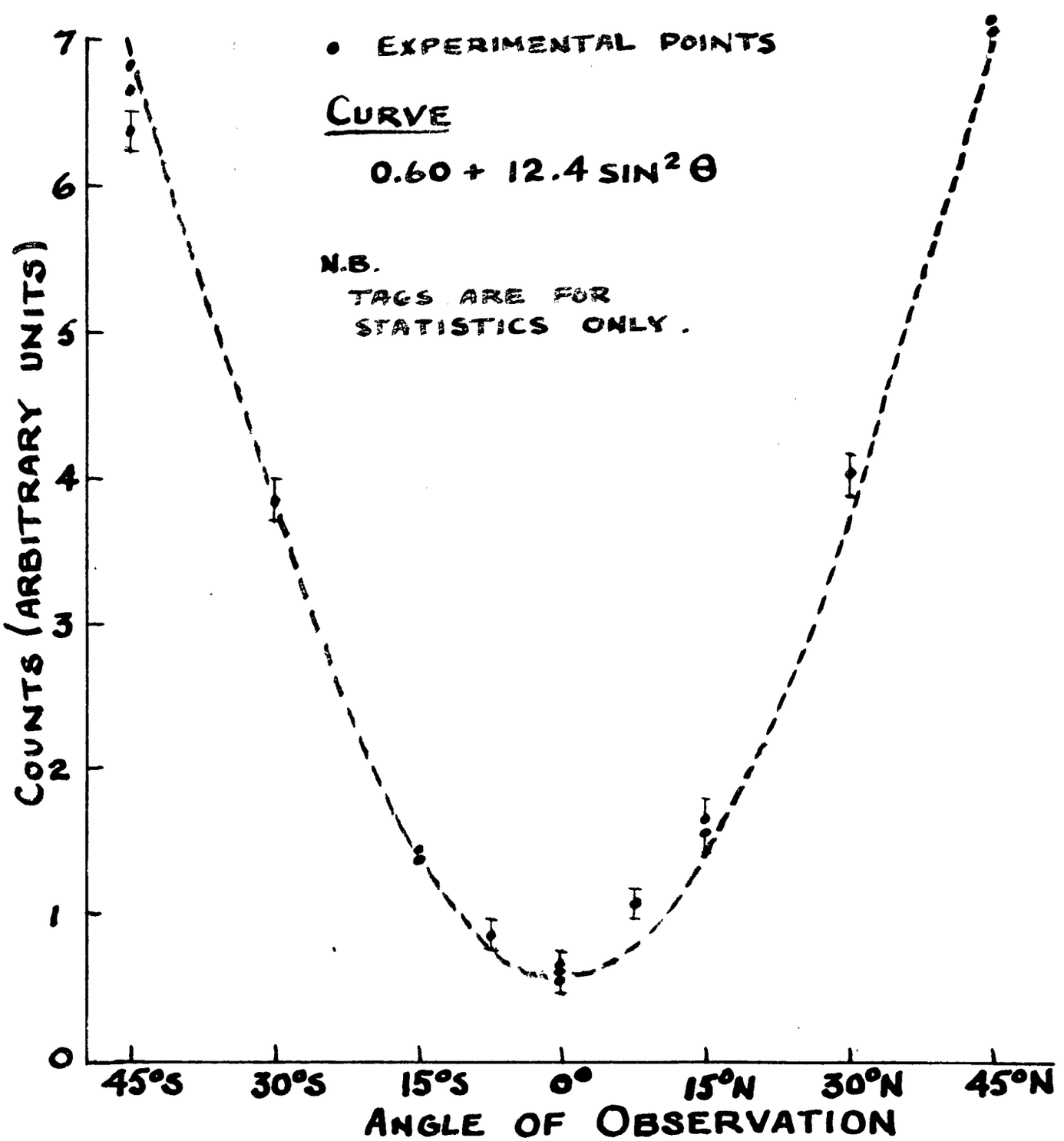

TABLE 4

Proton Energy	Experimental Angular Distⁿ Flux/Unit Solid	Solid Angle Corrⁿ	Neutron Corrⁿ	Corrected Angular Distⁿ	% Isotropic Yield
1.75 Mev.	$\sin^2\theta+(.047 \pm .005)$	-.010	-.012 ± .005	$\sin^2\theta+(.025 \pm .007)$	3.6 ± 0.9
1.0 Mev.	$\sin^2\theta+(.069 \pm .004)$	-.010	-.016 ± .007	$\sin^2\theta+(.043 \pm .008)$	6.1 ± 1.0

25% ± 10% of the counts in the 0° direction were caused by neutrons. The neutrons arose from bombarding the target but no complete explanation for the mechanism of their production has yet been advanced.

e) Excitation Function

The main counter was placed in the 90°S position. The target and beam were then lined up as previously described. A known mass of D_2O was injected into the chamber, forming a solid ice target on the backing. A proton beam of energy 1.25 Mev. was focussed on this target. The time, kick-sorter spectrum, and integrated number of counts above a bias level of 4.25 Mev., were recorded for a know integrated beam current striking the target.

The energy of the beam was raised and the same data recorded at the higher energy. Three or four sets of readings were taken at energies above 1.25 Mev. and then a set of readings was again taken at 1.25 Mev. This procedure was continued until sixteen readings at nine different energies (in addition to those at 1.25 Mev.) had been obtained. The highest was at 1.86 Mev. Then two sets of readings were taken at 1.25 Mev. and one at 1 Mev. For readings below 1 Mev. the point at 1 Mev. was used as a check point and it was repeated every fourth time or less. The lowest proton energy used was 250 kev. This was obtained by using the 500 kev. singly-charged hydrogen molecules (mass 2 beam). One run was done with the 1 Mev. mass 2 beam to check the consistency of measurements made with the mass 2 beam and

the mass one beam at half the energy. Of course the readings taken with the mass 2 beam were normalized to $\frac{1}{2}$ the integrated current used for the other readings. At all points other than those mentioned above the mass 1 beam was used.

The target was then removed by heating, and background were taken over the same range of energies. Backgrounds were taken at the same energy as most of the points but there were a few exceptions which will be noted later. For the backgrounds, the time, integrated current, kick-sorter spectrum and integrated counts above 4.25 Mev. were recorded.

Five counter checks, using a RaTh source, were spaced evenly throughout the other readings to insure that the energy calibration did not shift appreciable. One small shift occurred and was immediatly corrected. Since the check points were used to normalize the counts no additional corrections were required due to this small shift.

Cosmic ray backgrounds which had previously been measured for the counter were used in treating the results.

Treatment of Data

The cosmic ray background associated with the time taken for each reading was subtracted from the integrated counts above 4.25 Mev. for all readings. The set background (i.e. all background other than cosmic ray) was subtracted from the D_2O readings at each energy, the integrated beam current being used for normalization.

It was found that the counts at the check points decreased as more points were taken. Presumably this was due to a loss of D_2O as the target was bombarded. It was assumed that the loss of D_2O per point between any two check points was a constant. Corrections were determined at each check point to make the readings at all check points consistent. The intermediate points were then corrected in line with the assumption made above. The results appear in table 5 under experimental results and are plotted in fig. 13.

Results

TABLE 5

Ep Mev.	dE Mev.	Ep Mev.	E Mev.	K%	Relative Yield Exp't'l Results	Relative Yield Corrected Results
0.250	0.17	.17±.06	5.60	29.2%	0.412	0.470
0.500	0.111	.44±.04	5.79	31.1	2.03	2.17
0.750	0.087	.71±.03	5.96	32.2	3.25	3.36
1.00	0.070	.97±.03	6.14	33.3	4.00	4.00
1.26	.058	1.23±.03	6.31	34.2	4.90	4.77
1.32	.055	1.29	6.37	34.5	4.86	4.69
1.40	.053	1.37	6.42	34.7	5.70	5.47
1.48	.052	1.45	6.46	34.9	5.29	5.05
1.53	.050	1.50	6.49	35.1	5.68	5.39
1.58	.049	1.56	6.52	35.3	5.62	5.30
1.66	.047	1.64	6.58	35.6	5.74	5.37
1.75	.045	1.73	6.64	35.9	6.13	5.69
1.80	.044	1.78	6.68	36.1	6.48	5.98
1.86	.043	1.84	6.72	36.3	6.32	5.80

Column one shows the incident proton energy. This was determined using an energy scale set up by a study of fluorine resonances. (10)

Column two is the target thickness in Mev. at each energy. This was determined as is shown later.

FIG. 13.

EXCITATION FUNCTION FOR THE REACTION $H^2(p,\gamma)He^3$

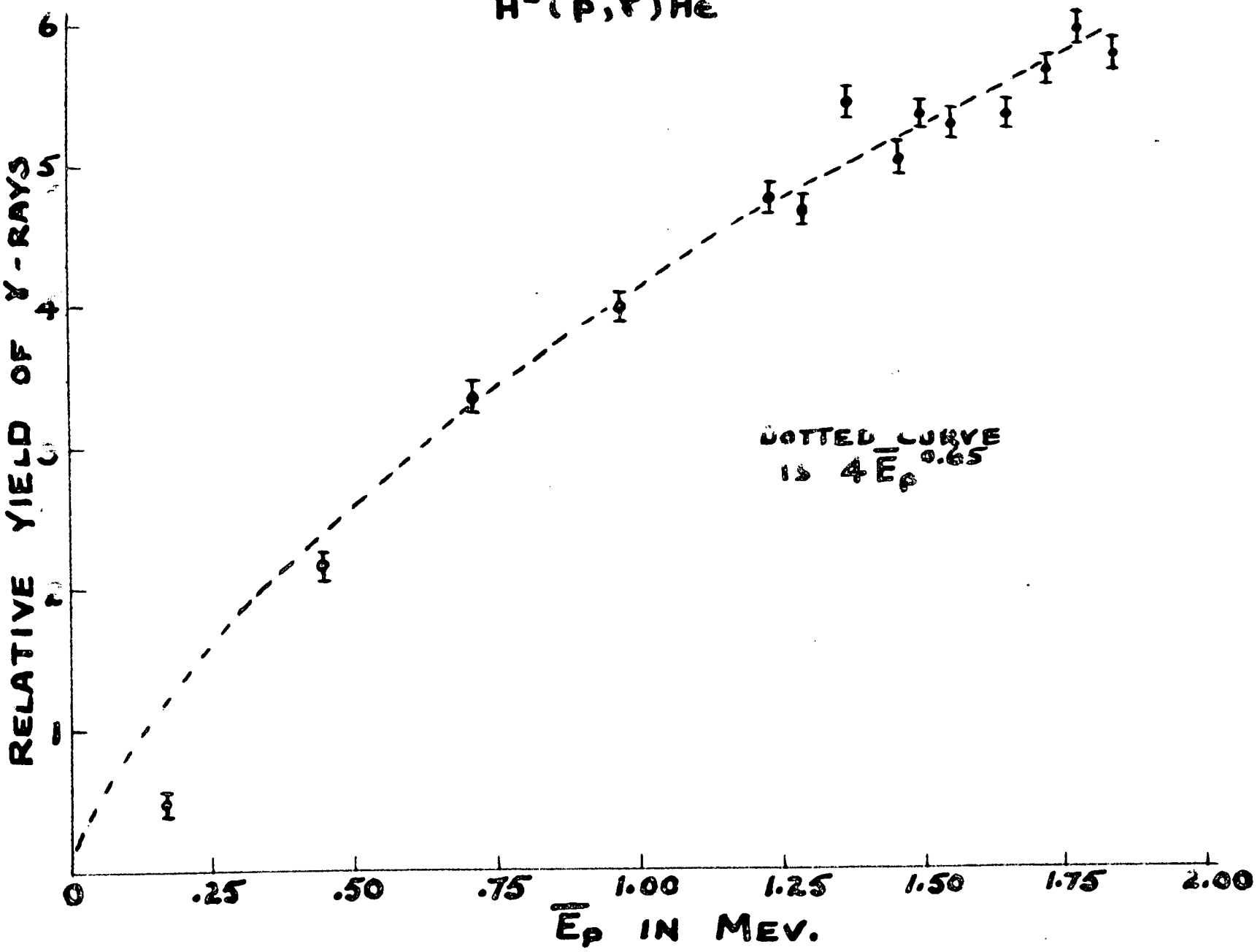

Column three is the average proton energy, while in the target, for protons going through the target.

Column four is the average gamma ray energy associated with the average proton energy.

Column five is the counting system efficiency. This is normalized at 33.3% at 1 Mev. which is the approximate absolute value at that energy. A sample calculation is given below showing how these efficiencies were obtained.

Column six shows the exp't'l results as treated above.

Column seven shows the final results corrected for counter efficiency.

Sample Calculations

i) Target thickness as a function of energy

250 c.c. of D_2O vapour at 1.3 cms. of mercury press. was injected.

$$\text{Mass of } D_2O \text{ injected} = \frac{250}{22{,}000}\,\frac{1.3}{76}\,(20) = .00388\text{g.}$$

It is assumed that this spread over a hemisphere of radius 2 cm.

$$\text{Thickness} = \frac{.00388}{(2)^2} = .00032\text{g/cm}^2$$

At Ep = 500 Kev. (15)

$$\epsilon = \text{stopping } X^{n} = 11.6 \times 10^{-15} \text{ ev-cm}^2$$

$$\text{At 500 kev. } dE = \epsilon N dX$$

$$= (11.6 \times 10^{-15}) \times .00032 \times \frac{6 \times 10^{23}}{20}$$

$$= 11.1 \times 10^{4} \text{ ev.}$$

$$= 0.111 \text{ Mev.}$$

Stopping numbers [17] were used in ranges where stopping cross-sections were not tabulated.

Counter efficiencies

The cross-sections for the various absorption processes as a function of energy were obtained by interpolating between published values. [12]

The ratio of the efficiency at Ep = 1.86 Mev. to that at Ep = 1.00 Mev. is as obtained in the following manner.

Ep Mev.	$\overline{E_\gamma}$ Mev.	$\sigma_{Comp.}$ barns	$\sigma_{Tot.}$ barns.
1.86	6.72	3.534	7.714
1.00	6.14	3.820	7.676

Since the bias is set at 4.25 Mev. many of the counts arising from Compton absorption do not register. An estimate of the proportion of those which are absorbed by the Compton process which do not register is given $\frac{\overline{E_\gamma} - 4.25}{\overline{E_\gamma}}$

$$\frac{\text{Efficiency at } \overline{E_\gamma} = 6.72 \text{ Mev.}}{\text{Efficiency at } \overline{E_\gamma} = 6.14 \text{ Mev.}} = \frac{7.714 - \frac{4.25}{6.72}(3.534)}{7.676 - \frac{4.25}{6.14}(3.820)}$$

$$= \underline{1.089.}$$

If the efficiency at 6.14 Mev. is 33.3%

Then the efficiency at 6.72 Mev. is 36.3%

An approximate estimate of the efficiency at $\overline{E_\gamma}$ = 6.14 Mev. is obtained as follows:

Effective macroscopic X^n at $\overline{E_\gamma}$ = 6.14 Mev.

$$= \left\{\left[7.676 - \frac{4.25}{6.14}(3.820)\right] \times 10^{-24}\right\} \frac{(6.02 \times 10^{23})(3.67)}{126}$$

$$= .088 \text{ cm}^{-1}$$

Capture mean free path = 11.4 cm.

Approx. av'g. effective path in crystal = 4 cm.

$$\text{Efficiency} \times 1 - e^{\frac{-4}{11.4}} \approx .333$$

V. Sources of Error

i) Angular Distributions

There was one correction which was not applied to the angular distribution as it could not be done accurately. However it was checked that its magnitude was small.

For a given incident proton energy, the gamma ray energy was a weak function of angle of observation due to the Doppler Shift. Hence the counter efficiency was also a weak function of angle. This was accentuated by the fact that a fixed bias was used. It was estimated that the counter efficiency changed by about 3% between 0^{o} and 150^{o} at Ep = 1 Mev., and by 5% between the same angles of observation at Ep = 1.7 Mev.

The direction of the correction would be to lower points at angles less than 90^{o} and raise them at angles greater than 90^{o}. It is interesting to note that such a correction would tend to make the agreement between the experimental points and a curve of the form, $a + b \sin^{2}\theta$, better in figure 11. However it will not seriously change the ratio of a to b.

The relativistic correction relating angles in the observer's system to angles in the centre of mass system would also tend to better agreement. This correction would tend to shift the peak of the distribution to about 87^{o} at 1 Mev. This correction has not been shown in detail since it is small compared to the statistics on the points.

ii) Excitation Function

This part of the work was the least accurate for two reasons

Firstly there were fairly large changes in counting efficiency over the region studied, which had to be estimated. Secondly the current integrator had to be relied upon in order to normalize results to the same numbers of incident particles. It was found when working at constant incident particle energy, where the monitor counts were also available for normalization, that this was not always completely reliable. This was probably due to slight shifts of the beam on the target to a slightly different thickness of target. However, enough check points were taken to guarantee 5% accuracy provided the current integrator normalization was as good as experience at constant incident particle energy led us to believe.

VI. Conclusions

1. The gamma ray energy in the reaction, $H^2(p,\gamma)He^3$, is given by,

$$E_\gamma = Q + (2/3)Ep$$

where E_γ is the gamma ray energy

Ep is the incident proton energy

and $Q = 5.50 \pm 0.03$ Mev.

Since this value for Q agrees, within experimental error, with the latest published figures for the mass difference between $H^2 + p$ and He^3, the gamma ray transition must lead directly to the ground state of He^3.

2. Since the measured and calculated values for Doppler Shift in gamma ray energy agree, the time between proton absorption and gamma ray emission must be short compared to the average slowing down time of a deuterium molecule in deuterium. (i.e. $< 2 \times 10^{-12}$ sec.)

3. There is an isotropic component (or at least a component at 0^o) to the angular distribution of gamma rays. Therefore the gamma rays are not completely polarized. The percentage of isotropic component is a function of energy. The measured distribution functions were:

At 1.75 Mev.

$$y(\theta) = \sin^2\theta + (.025 \pm .007)$$

At 1.00 Mev.

$$y(\theta) = \sin^2\theta + (.043 \pm .008)$$

4. The excitation function shows no obvious resonances but is a continually rising function over the range of incident proton energies studied. Over the range from 500 Kev. to 1.85 Mev.

the experimental points are fit by a function of the form,

$y = AE^{0.65}$,

where A is an undetermined constant,

E is the incident proton energy.

VII. BIBLIOGRAPHY

1. Wilkinson, D.
   Phil. Mag., 43, 659, (1952)

2. Fowler, Lauritsen and Tollestrup.
   Rev. Mod. Phys. 78, 1767, (1949)

3. Fowler et al.,
   Rev. Mod. Phys. 22, 291, (1950)

4. Ajzenburg and Lauritsen
   Rev. Mod. Phys. 24, 321, (1952)

5. Heitler, W (1944)
   "The Quantum Theory of Radiation" (Second Edition),
   Oxford University Press, London.

6. French, A.
   Mimeographer Lecture Notes, Cavendish Laboratory,
   Cambridge University, (1950)

7. M. Verde
   Helv. Phys. Acta 23, 453, (1950)

8. D. Aaronson,
   M.A.Sc. thesis, UBC, (1950)

9. F. Flack,
   Ph.D. thesis, UBC, (1951)

10. D. Aaronson,
    Ph.D. thesis, U.B.C., (1952)

11. S. Woods,
    Ph.D. thesis, U.B.C., (1951)

12. Davisson and Evans,
    Rev. Mod. Phys. 24, 79, (1952)

13. R. Azuma,
    M.A. thesis, U.B.C., (1951)

14. Moody, N., Howel, W., Battell, W., and Taplin, R.
    Rev. Sci. Inst. 22, 551, (1951)

15. Wenzel and Whaling,
    Phys. Rev., Aug. 1, 1952, P. 501

16. Hornyak, Lauritsen, Morrison and Fowler.
    Rev. Mod. Phys. 22, 357, (1950)

17. Herschfelder and Magee.
    Phys. Rev. 73, 207, (1948)

Appendix A

Solid Angle Correction at $\theta = 0^{o}$ for a $\sin^2\theta$ Distribution.

Suppose the actual flux distribution of gamma rays, $y(\theta)$, is given by,

$$y(\theta) = A \sin^2\theta$$

If the counter used in measuring the distribution subtends a finite angle at the source, the measured distribution will not be zero at $\theta = 0^{o}$.

Let F be the ratio of counts recorded at 0^{o} to those recorded at 90^{o},
R be the effective radius of the detection crystal
l be the effective distance from the source to the detecting crystal.

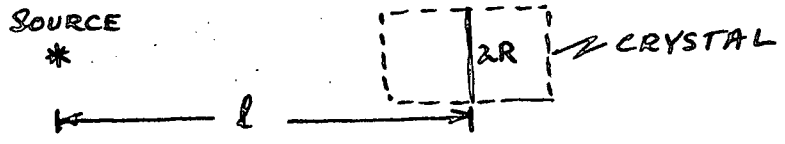

If $\frac{R}{l}$ is small compared to one,

Then

$$F \approx \frac{2\pi A l^2 \int_0^{\theta(R)} \theta \sin^2\theta \, d\theta}{2\pi A l^2 \int_0^{\theta(R)} \theta \, d\theta}$$

where $\theta(R) = \tan^{-1} \frac{R}{l}$

For small θ , $\theta \approx \sin \theta$

$$F \approx \frac{\int_0^{\theta(R)} \theta^3 d\theta}{\int_0^{\theta(R)} \theta^3 d\theta} = \frac{\theta^2(R)}{2}$$

In our angular distributions,

$$\theta(R) = \tan^{-1} \frac{.87}{6} = .144 \text{ radians}$$

$$\therefore F = .0104$$

More accurate considerations, in which the assumption that $\Theta(R)$ is small is not made, show that this value is good to better than 3%. Hence the above value was used in our work for the solid angle correction for $\theta = 0^{o}$.